A neutron diffraction study of the magnetic phases of $CsCuCl_3$ for in-plane fields up to 17 T

2002 J. Phys.: Condens. Matter 14 5161

(http://iopscience.iop.org/0953-8984/14/20/311)

INSTITUTE OF PHYSICS PUBLISHING JOURNAL OF PHYSICS: CONDENSED MATTER

J. Phys.: Condens. Matter **14** (2002) 5161–5172 PII: S0953-8984(02)33468-4

A neutron diffraction study of the magnetic phases of $CsCuCl_3$ for in-plane fields up to 17 T

N Stüßer[1], U Schotte[1], A Hoser[1,2], M Meschke[1], M Meißner[1] and J Wosnitza[3]

[1] Hahn-Meitner Institut, D-14109 Berlin, Germany
[2] Institut für Kristallographie, RWTH-Aachen, Aachen, Germany
[3] Institut für Angewandte Physik, TU-Dresden, D-01062 Dresden, Germany

E-mail: stuesser@hmi.de

Received 5 February 2002, in final form 11 April 2002
Published 9 May 2002
Online at stacks.iop.org/JPhysCM/14/5161

Abstract

Neutron diffraction investigations have been performed to study the magnetization process of $CsCuCl_3$ with the magnetic field aligned within the ab-plane. In zero field the stacked, triangular-lattice antiferromagnet (TLA) $CsCuCl_3$ has a helical structure incommensurate in the chain direction normal to the ab-plane. The magnetic phase diagram was investigated from 2 K up to T_N in fields up to 17 T. The phase line for the expected incommensurate–commensurate (IC–C) phase transition could be determined throughout the whole phase diagram. At low temperature the IC–C transition is roughly at half the saturation field H_S. The neutron diffraction patterns were found to be well described by a sinusoidally modulated spiral in fields up to $H_S/3$. The initial increase of the scattering intensity in rising field indicates a continuous reduction of the spin frustration on the triangular lattice. Between $H_S/3$ and $H_S/2$ a new phase occurs where the spiral vector has a plateau in its field dependence. Close to the IC–C transition a growing asymmetry of magnetic satellite-peak intensities indicates domain effects which are related to the lifting of the chiral degeneracy in the ab-plane in rising field. The phase diagram obtained has some similarities with those calculated for stacked TLAs by considering the effects of quantum and thermal fluctuations.

1. Introduction

$CsCuCl_3$ is a hexagonal perovskite which undergoes a structural phase transition at 423 K due to the cooperative Jahn–Teller effect of the Cu^{2+} ion. The lattice symmetry changes from $P6_3/mmc$ to $P6_122$ in the low-temperature phase [1]. The lattice consists of chains of face-sharing distorted Cl_6 octahedra centred on the Cu^{2+} ions along the c-axis. These chains are arranged on a triangular lattice in the ab-plane.

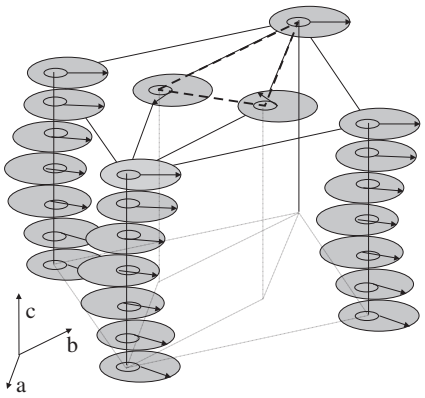

Figure 1. A sketch of the magnetic structure of $CsCuCl_3$ in zero field. The spiralling of the Cu^{2+} ions at the Wyckoff position 2a (with $x = 0.06$) around the c-axis, indicated by the small circles, is exaggerated. The 120° rotation of neighbouring spins on a triangular plaquette is indicated by the broken line.

Long-range magnetic order of the Cu^{2+} moments occurs below 10.65 K [2]. A triangular spin arrangement of the 120°-type structure is formed in the ab-plane and an incommensurate spiral along the c-axis with a repetition length of about 71 layers (figure 1). The 120° structure results from the antiferromagnetic coupling on the triangular lattice. $CsCuCl_3$ belongs to the family of frustrated magnetic systems. The reduction (to 0.58 μ_B) of the ordered moment of the $S = 1/2$ spin of the Cu^{2+} ion is not uncommon in frustrated triangular-lattice antiferromagnetic (TLA) systems. The magnetic interaction along the c-axis is predominantly ferromagnetic. An additional Dzyaloshinskii–Moriya interaction—possible by the low symmetry in the local structure due to the Jahn–Teller distortion—accounts for the observed incommensurate magnetic helix along the c-axis.

Anomalies in the field-dependent magnetization at low temperatures [3]—a small step in the magnetization for a field parallel to c and a 'shoulder' for the in-plane field—have stimulated many experimental and theoretical studies during the last decade. It is now understood that these anomalies, which cannot be accounted for by classical theory, are a consequence of the influence of quantum fluctuations at low temperatures and thermal fluctuations at higher temperatures [4–7]. Therefore, $CsCuCl_3$ is one of the rare systems where extraordinarily large effects of fluctuations on the magnetic structure can be studied. In particular, the phase diagrams in the H–T plane show various magnetic structures which, in addition, depend strongly on the direction of the applied field.

The behaviour of the spin arrangement in a magnetic field aligned along the c-axis [8] seems to be basically understood using linear spin-wave theory [4] or Monte Carlo calculations [9]: quantum or thermal fluctuations induce a first-order transition from the so-called 'umbrella' structure favoured by an in-plane anisotropy to a 2–1 structure in which two spins are parallel and the third one is oriented such that the sum of the moments of the sublattices is parallel to the field.

A more complex magnetic behaviour is found for the transverse-field case. Magnetization measurements at 1.1 K using pulsed-field techniques show a linear $M(H)$ dependence up to 10.5 T. Between 10.5 and 14.5 T $\mathrm{d}M/\mathrm{d}H$ is reduced significantly (plateau) and it increases again above 14.5 T with the magnetization approaching saturation linearly at about 31 T [3]. In magnetoacoustic studies at 1.5 K the longitudinal sound velocity c_{11} reveals a broad anomaly between 12 and 17 T and a step-like anomaly near 34 T [10]. Further indication of a magnetic

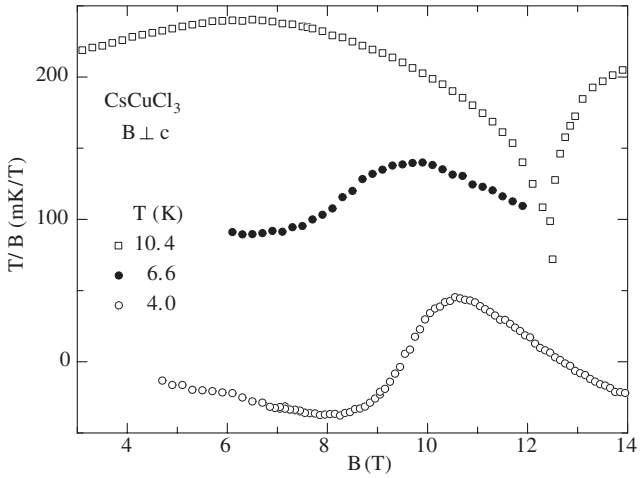

Figure 2. The magnetocaloric effect $\Delta T/\Delta B$ of $CsCuCl_3$. Data at 6.6 and 10.4 K are shifted by 100 and 200 mK T^{-1}, respectively (from [11]).

phase transition at fields around 9 T in the range between 4 and 7 K was recently confirmed by magnetocaloric effect data [11]. In figure 2, for the data at 4.0 and 6.6 K the point of inflection between the broad minima and maxima in $\Delta T/\Delta B$ versus B is ascribed to the transition field. Pioneering neutron work on magnetic phase transitions in $CsCuCl_3$ has been done at a spallation source. The magnetic propagation vector $\boldsymbol{q} = \langle 1/3, 1/3, Q\rangle$ was determined in high pulsed fields and shown to go to $\langle 1/3, 1/3, 0\rangle$ near 17 T [12]. All these measurements point to the existence of two incommensurate magnetic phases denoted by IC1 and IC3 and a commensurate phase C, besides the fluctuation-induced incommensurate phase IC2 which was studied earlier [13]. Up to now a complete phase diagram in the H–T space like the one determined by the present work (see figure 8 below) has not yet been published.

More quantitative neutron diffraction studies allowing a better insight into the microscopic structure of the different phases were impeded by the lack of the necessary high magnetic fields. The availability of the superconducting VM1 magnet in connection with a dysprosium booster at the Berlin Neutron Scattering Centre (BENSC) enabled us to study the magnetic phases including the IC3–C transition throughout the whole H–T phase diagram. We, in addition, performed measurements of $M(H)$ by superconducting quantum interference device (SQUID) magnetometry for the study of the IC1–IC3 transition.

2. Experimental results

The diffraction experiments were carried out at the E1 triple-axis spectrometer at BENSC with the analyser removed. The wavelength used was 2.4 Å provided by a pyrolytic graphite monochromator. The second-order contamination $\lambda/2$ was suppressed by a pyrolytic graphite filter and the collimations $\alpha_1, \alpha_2, \alpha_3$, and α_4 were set to open, 20′, open, and open, respectively. This allowed a reasonable resolution with good intensity at the desired small diffraction angles. The samples were single crystals of $CsCuCl_3$ grown from solution. They have a hexagonal shape with cross section of about 12 mm^2 and length of 6 mm.

The field-dependent measurements were performed using the 14.5 T superconducting magnet VM1 equipped with a Dy booster enhancing the maximum available field to 17 T. This booster consists of two Dy pole pieces providing an additional field strength of 2.5 T.

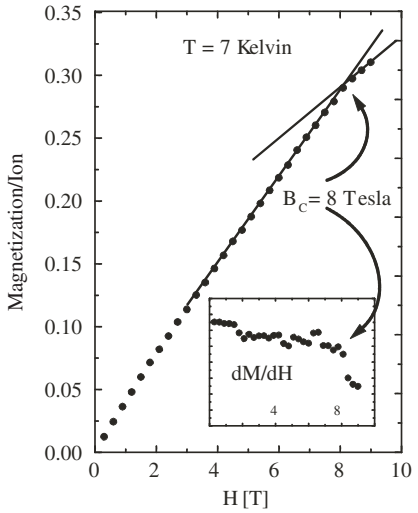

Figure 3. The magnetization curve $M(H)$ of $CsCuCl_3$ measured by SQUID magnetometry at 7 K. The kink in dM/dH at the IC1–IC3 transition is clearly visible at 8 T.

The accuracy of the field calibration is about 0.1 T. The sample was put into an Al holder sandwiched by the Dy and the whole set-up was inserted into the sample space. The Dy booster actually limits the sample volume to the dimensions stated above. Field inhomogeneities were estimated to be about 0.1 T. The sample was mounted with the $(h\ h\ l)$ zone in the scattering plane so that the vertical field was within the ab-plane and the field along one of the sixfold-degenerate $\langle 1\ 0\ 0\rangle$ directions. During the field experiments the nuclear reflections 1 1 0 and 0 0 1 were measured repeatedly to control for the correct orientation of the sample. The bulk magnetization was measured by SQUID magnetometry in fields up to 9 T. Thereby, the temperature was controlled within 15 mK.

In the following we present our results from magnetic neutron diffraction and from magnetization measurements. The volume magnetization directly provides the average moment along the field direction while neutron diffraction probes the Fourier components for periodic spin arrangements. Our magnetization measurements at different temperatures show some general features: one observes a linear increase of $M(H)$ up to about $H_S/3$ followed by a kink with a significantly reduced dM/dH (figure 3). We find that the measured $M(H)$ curves are only weakly dependent on temperature between 1.8 and 10 K. The reduction in magnetization is about 5% at 10 K referred to the measurement at 1.8 K.

While in the SQUID measurement only the IC1 and IC2 phases were accessible, all three phases, IC1, IC3, and C, could be studied in our neutron diffraction scans along $\langle 1/3, 1/3, l\rangle$ measured at various temperatures in the range between 2 and 10.5 K and in fields up to 17 T.

2.1. Low-field phase IC1

In zero field, magnetic Bragg intensities can be detected at $1/3\ 1/3\ \pm Q$ originating from the triangular spin arrangement in the ab-plane and the regular spiral along c (figure 4). In the IC1 phase the z-component Q of the magnetic propagation vector $\boldsymbol{q}$ decreases continuously with applied field and new magnetic satellites occur at $1/3\ 1/3\ \pm 2Q$ (see figure 4 for $H = 6$ T).

Moreover, one observes an increase in intensity of the magnetic Bragg reflections with rising field which is more pronounced at higher temperatures, but also clearly observed at 2 K.

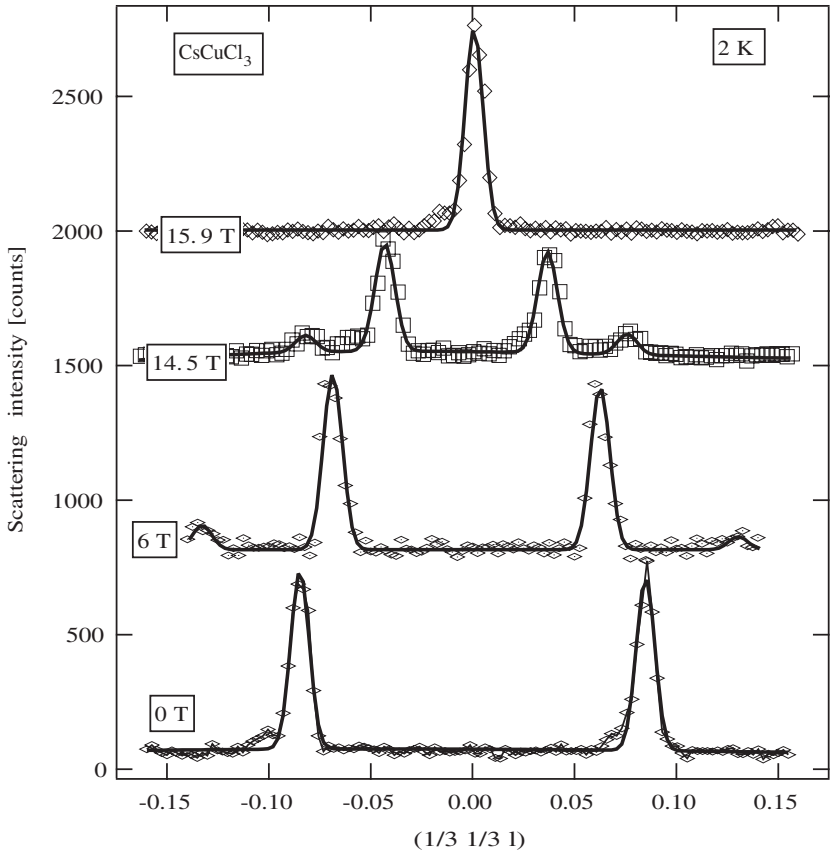

Figure 4. Diffraction patterns along $\langle 1/3, 1/3, l\rangle$ at different fields for one sample in the C phase (15.9 T), the IC3 phase (14.5 T), and the IC1 phase (6 and 0 T). The data are shifted consecutively by different amounts.

This is shown in figure 5 together with the field dependence of Q and of the intensity ratio $I(1/3\ 1/3\ \pm 2Q)/I(1/3\ 1/3\ \pm Q)$. The measurements in IC1 below 11 T did not give any indication of reflections at $1/3\ 1/3\ 0$ and $1/3\ 1/3\ \pm nQ$ with n from 3 to 6.

2.2. Intermediate-field phase IC3

Around the kink in $M(H)$ the propagation vector enters a region of saturation with $Q \approx 0.05$. This value of Q is found at all temperatures between 2 and 10.5 K (figure 6). At the boundary between IC1 and IC3 the magnetic Bragg intensities show a maximum followed by a decrease of the intensity over the whole range of stability of the phase IC3. The intensity ratio of the magnetic satellites at $1/3\ 1/3\ \pm Q$ and $1/3\ 1/3\ \pm 2Q$ stays approximately constant (figure 5). In the phase IC3 no peaks at $1/3\ 1/3\ \pm nQ$ for $n = 3$ and 4 were visible. A change in the magnetic behaviour compared to that for low and intermediate fields is further indicated by an increase of the linewidth of about 20%. The linewidth of the magnetic reflections in the phase IC1 is approximately given by the instrumental resolution and the mosaicity of the sample.

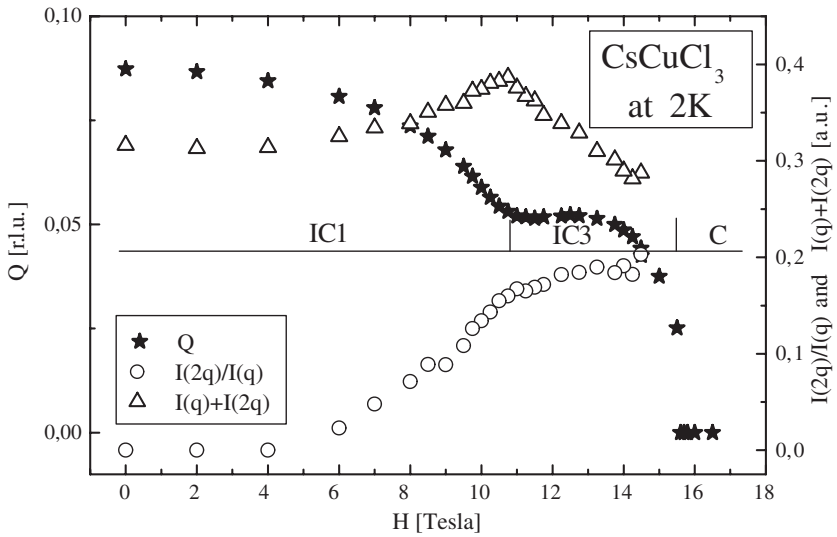

Figure 5. The field dependence of the integrated peak intensities $I(1/3\ 1/3\ \pm Q)$ + $I(1/3\ 1/3\ \pm 2Q)$, the intensity ratio $I(1/3\ 1/3\ \pm 2Q)/I(1/3\ 1/3\ \pm Q)$, and $Q(H)$ measured at 2 K. The stability regions for the phases IC1, IC3, and C are indicated.

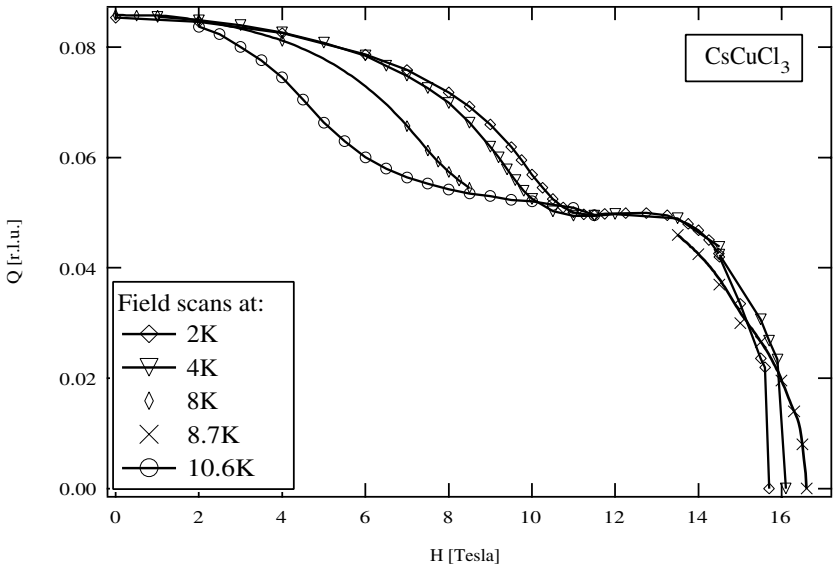

Figure 6. The spiral component $Q(H)$ along c at different temperatures. The plateau at $Q \approx 0.05$ in the phase IC3 is clearly visible.

2.3. High-field phase C

Close to the upper field boundary of the IC3 phase, $Q(H)$ decreases again and a new phase is observed as indicated by a $1/3\ 1/3\ 0$ reflection, while those at $1/3\ 1/3\ \pm Q$ and $1/3\ 1/3\ \pm 2Q$ disappear (figures 4 and 7). At 2 K this happens at 15.6 T. The new phase is commensurate, i.e., the spirals along c disappear. The phase transition occurs within a field interval of 0.2 T. In this

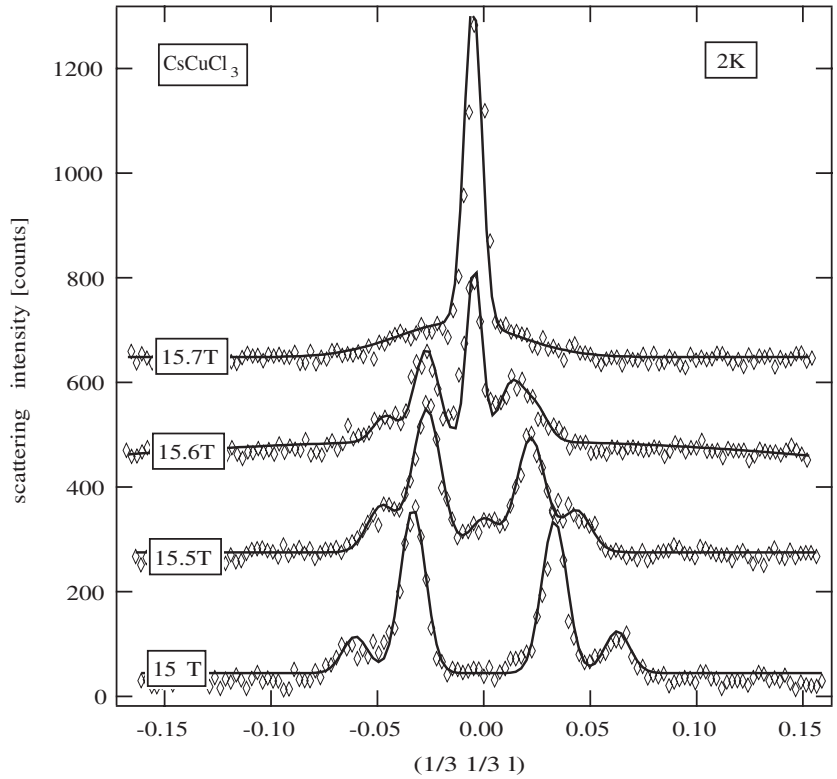

Figure 7. Diffraction patterns along $\langle 1/3, 1/3, l\rangle$ across the IC3–C phase transition. Note the asymmetry in the peak intensities and the coexistence range around 15.6 T. The data are shifted consecutively by different amounts.

small field region we observe a coexistence of the phases IC3 and C. It cannot be decided yet whether this coexistence reflects the presence of field inhomogeneities (see above) or whether it is related to a two-phase regime characteristic of a first-order transition. No hysteresis was found by cycling the sample through the IC3–C transition with rising and falling field. The linewidth of the magnetic reflection $1/3\ 1/3\ 0$ is mainly resolution limited like in the IC1 phase.

What is remarkable is the appearance of an asymmetry between the peak intensities at $1/3\ 1/3 + Q$ and $1/3\ 1/3 - Q$ and—with reversed sign—between those at $1/3\ 1/3 - 2Q$ and $1/3\ 1/3 + 2Q$. This asymmetry was found to be more or less pronounced for different samples and develops with increasing field strength close to the IC3–C phase transition. It generally occurs in rising fields above 14.5 T, but remains with slightly weaker asymmetry upon field reduction. After cycling the sample through T_N at zero field the two peaks at $1/3\ 1/3 + Q$ and $1/3\ 1/3 - Q$ have equal intensity again. The asymmetry can occur in both directions as observed for the same sample in field scans at different temperatures. Systematic investigations to clarify this behaviour are planned. Nevertheless, in the next section we will sketch magnetic structure factor calculations which explain the phenomenon as a domain effect of the chirality within the *ab*-plane.

A phase diagram has been determined from all our measurements in the H–T space (figure 8). Included in this figure are the results of the bulk measurements mentioned in the introduction. We also show the boundaries of the phase IC2, which develops very close to the paramagnetic region and which was studied by us earlier [6, 11, 13].

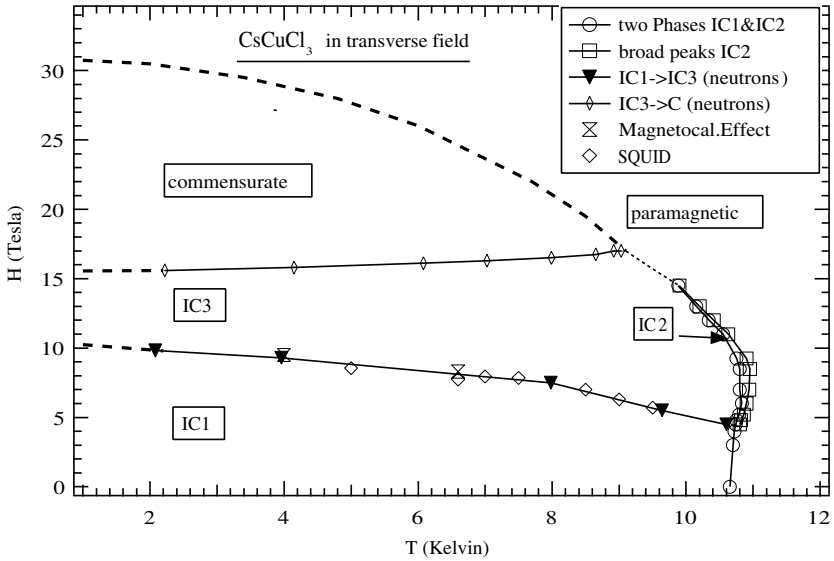

Figure 8. The magnetic phase diagram of $CsCuCl_3$. The thin broken curve marks a boundary where different phases could not be resolved in the diffraction pattern. Thick broken curves mark the extrapolation of our data to lower T. The paramagnetic boundary is taken from [3].

3. Discussion

In the following, we will interpret our observations with regard to the spin arrangements during the magnetization process and we will compare our results with theoretical predictions for magnetically frustrated AF systems on triangular lattices.

3.1. Low-field phase IC1

The regular magnetic spiral at zero field is described by one of the magnetic propagation vectors $\langle 1/3, 1/3, \pm Q\rangle$ with a moment of 0.58 μ_B on the Cu^{2+} ion [2]. At low field strength, still within the IC1 phase, the spirals show a distortion indicated by the presence of the reflections $1/3\ 1/3 \pm Q$ and $1/3\ 1/3 \pm 2Q$ [13], consistent with a sinusoidal modulation. This behaviour can be understood from conventional mean-field theory [5,7]. The predicted decrease in Q with increasing field reflects the elongation of the spirals and agrees—at least qualitatively—with the measured $Q(H)$. An unexpected feature is the rise of all diffraction intensities observed in the phase IC1. This shows that the Fourier components of the ordered magnetic moment increase with applied field. At the lowest temperature measured (2 K) this may be explained by the fact that the ordered spins on the triangular frustrated lattice suffer a large moment reduction which reduces in an external field, i.e., the frustration gets partially lifted. Magnetization measurements of the paramagnetically saturated state at 1.1 K determined indeed a moment of 1.1 μ_B [3] which is about a factor of two larger than the ordered moment in the antiferromagnetic ground state [2]. At higher temperatures the rise in intensity is much more pronounced and one has to consider a reduction of the thermal fluctuations by the applied field as well. On the other hand we have to note that the linear increase of the magnetization with applied field in the IC1 phase (figure 3) was only weakly temperature dependent.

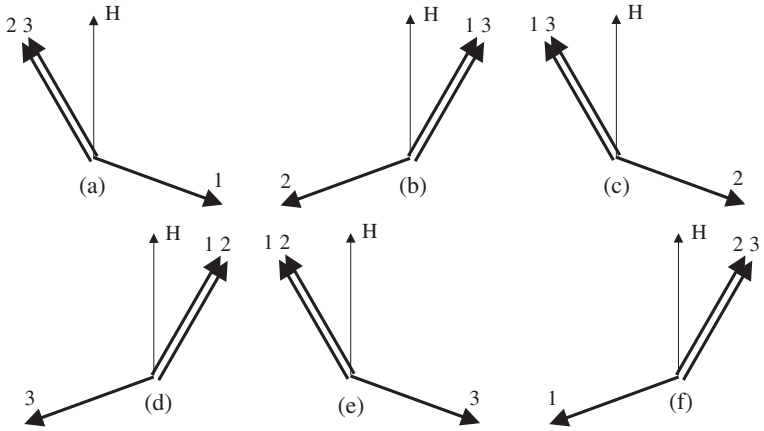

Figure 9. The model of the spin arrangement of the 2–1-type structure with a sequence of six domains as suggested for the IC3 phase.

3.2. Intermediate-field phase IC3

All observations point to a qualitative change of the spin structure at roughly 1/3 of the saturation field.

(i) The magnetic propagation vector becomes nearly independent of the field strength with decrease of the amplitudes of the Fourier components $1/3\ 1/3\ \pm Q$ and $1/3\ 1/3\ \pm 2Q$, keeping their intensity ratio roughly constant.

(ii) The magnetization increases with a reduced slope $\mathrm{d}M/\mathrm{d}B$ in comparison to the behaviour in IC1 (figure 3).

A quantitative analysis aimed at producing a description of this behaviour requires a model for the spin arrangement. It turned out that structure factor calculations for different spin models result in similar diffraction patterns with similar ratios of $I(1/3\ 1/3\ \pm Q)/I(1/3\ 1/3\ \pm 2Q)$. Moreover, consistent with our measurements, the Fourier components $1/3\ 1/3\ \pm nQ$ with $n = 0$ or n larger than 2 are only a few per cent of the dominant $1/3\ 1/3\ \pm Q$ reflection. The possibility of distinguishing the different models experimentally by means of different harmonics $1/3\ 1/3\ \pm nQ$ (remember that our scattering geometry is limited to the $(h\ h\ l)$ plane) is limited by the small sample space available in the 17 T magnet and the relatively small Cu^{2+} moment. Among the models tested was the sinusoidally modulated spiral theoretically predicted for low fields (figure 8 in [13]). Since earlier experiments on the magnetic structure in fields parallel to the c-axis showed a transition to a 2–1 structure favoured by fluctuations, a similar model [14] was tested too (figure 9). To account for the absence of a $1/3\ 1/3\ 0$ Fourier component this model consists of a sequence of six suitably different 2–1 domains separated by domain walls. An irregular arrangement of the domain walls could reduce the correlation length along the c-axis and perhaps account for the observed line broadening of the magnetic peaks. Similarly, the line broadening could also be caused by some irregularities in the spin arrangement within the distorted spiral. Since the data do not allow us to decide unambiguously between the different spin models, we will focus on the sinusoidal modulated structure in which the spin ordering is described by

$$\begin{aligned} S^x &= S_0 \cos(2\pi \mathrm{i}\boldsymbol{q}\cdot\boldsymbol{l} - \delta \sin(2\pi \mathrm{i}\boldsymbol{q}\cdot\boldsymbol{l})) \\ S^y &= S_0 \sin(2\pi \mathrm{i}\boldsymbol{q}\cdot\boldsymbol{l} - \delta \sin(2\pi \mathrm{i}\boldsymbol{q}\cdot\boldsymbol{l})) \end{aligned} \tag{1}$$

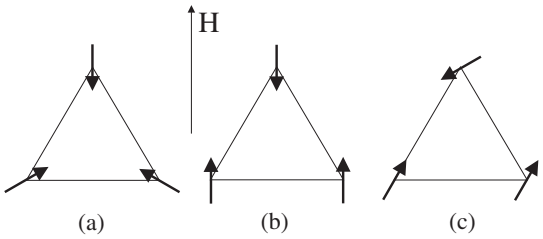

Figure 10. Three spin structures in transverse magnetic fields: (a) the chiral phase, (b) the collinear phase, and (c) the 2–1 spin-flop-like phase as is usually accepted to occur in stacked TLA magnets with increasing field.

with δ measuring the distortion of the spiral and $\boldsymbol{l}$ giving the positions of the magnetic ions. We have neglected the small positional spiralling of the Cu^{2+} ions around the c-axis. The effect of the modulation is to push the spins together in field direction and to spread them in the opposite direction [13]. Beyond $\delta = 1$, some spins close to the field direction turn backwards and the rise in $M(\delta)$ reduces significantly. The reduced magnetization $m = \langle S\rangle/S_0$ has a maximum around $\delta \approx 2$ with $m \approx 0.58$. Thus, for values of δ close to one and larger this structure will fail to give an appropriate behaviour of $M(H)$. The experiments show that the intensity ratio $I(1/3\ 1/3\ Q)/I(1/3\ 1/3\ 2Q)$ stays slightly below 4 which corresponds to $\delta = 1$. Apparently δ does not rise with field in the IC3 phase starting near $H_S/3$. For planar and stacked frustrated TLA the phase transition to a collinear and to the 2–1 phase (see figure 10) is well established. The spiral structure of the Cu^{2+} spins along the c-direction complicates the picture for $CsCuCl_3$.

The evolution of the peak asymmetry above 14.5 T shown in figure 7 points to domain formations. In the following we will give arguments indicating that these effects are related to domain formation in the ab-plane, but not along c. Earlier [13] we calculated the scattering intensity of distorted spirals, averaging over left- and right-handed spirals—what we might call the 'chain chirality'. We did not consider the second 'geometric chirality' in the ab-plane, i.e., the left- or right-handed 120° rotation of the three neighbouring spins on a triangular plaquette (see figure 1). As before, averaging over these two possible rotations reproduces the result in [13] and a symmetric intensity distribution at $1/3\ 1/3 \pm Q$ and $1/3\ 1/3 \pm 2Q$. In all our experiments we used samples which were selected to have a symmetric intensity distribution at zero field when cooled below T_N. If we now assume that the spiral turning sense, i.e., the 'chain chirality', is fixed by the crystal structure at the structural phase transition at 423 K, the evolving asymmetry in the field is connected with a change in the domain distribution of the 'geometric chirality'. The lifting of the degeneracy in the 'geometric chirality' near $H_S/3$ and the approach of an Ising-type phase transition has been described in [15] and we presume a connection to our observations. The scattering intensity for the case of an unbalanced distribution of domains of the geometric type of chirality is similarly calculated as described in [13]. Without averaging we obtain

$$\begin{aligned} I_q \propto S^2(1+\hat{k}_z^2)\sum_\tau \left\{ \frac{N_1}{N}\delta\left(\boldsymbol{k}+\left(\frac{1}{3},\frac{1}{3},Q\right)-\boldsymbol{\tau}\right)+\frac{N_2}{N}\delta\left(\boldsymbol{k}+\left(\frac{1}{3},\frac{1}{3},-Q\right)-\boldsymbol{\tau}\right)\right\} \\ + S^2\frac{\delta^2}{4}(1+\hat{k}_z^2)\sum_\tau \left\{ \frac{N_1}{N}\delta\left(\boldsymbol{k}+\left(\frac{1}{3},\frac{1}{3},-2Q\right)-\boldsymbol{\tau}\right) \right. \\ \left. + \frac{N_2}{N}\delta\left(\boldsymbol{k}+\left(\frac{1}{3},\frac{1}{3},2Q\right)-\boldsymbol{\tau}\right)\right\} \end{aligned} \tag{2}$$

for scans along $\langle 1/3, 1/3, l\rangle$. Here N_1 and N_2 give the occupancy of the two different domains with $N = N_1 + N_2$ being constant. If $N_1 = N_2 = N/2$ we reproduce the result given in [13]. If only one type of domain is present, e.g., only right-handed domains which might mean $N_2 = 0$, one sees directly that there are only peaks at $1/3\ 1/3\ Q$ and $1/3\ 1/3\ -2Q$. A similar consideration can be applied to the case where only left-handed domains are present ($N_1 = 0$) for which only peaks at $1/3\ 1/3\ -Q$ and $1/3\ 1/3\ 2Q$ appear. The observed asymmetry in our sample is most probably related to a redistribution in the domains with different types of the 'geometric chirality' caused by the external field. A similar domain effect was reported for $CsMnBr_3$—however, by using polarized neutrons [16]. At this point we want to stress clearly that our experiments using unpolarized neutrons cannot distinguish between the left- and right-handed helical structures with propagation vectors $\langle 1/3, 1/3, Q\rangle$ and $\langle -1/3, -1/3, -Q\rangle$, respectively. Instead we notice a difference between domains represented by $\langle 1/3\ 1/3\ Q\rangle$ or $\langle 1/3\ 1/3\ -Q\rangle$.

3.3. High-field phase C

The presence of the $1/3\ 1/3\ 0$ reflection and the absence of $1/3\ 1/3 \pm nQ$ reflections are strong evidence for a parallel alignment of the spins on the chains along c. In the ab-plane there are still three different sublattices. Again we are faced with the problem that the moment reduction in the field is unknown and the determination of the relative orientation of the three sublattices is uncertain. It seems to be generally accepted that fluctuations select the 2–1 structure from all degenerate configurations with equal average magnetization. Now there are six domains possible.

The phase diagram derived from our experiments resembles that of the frustrated ferromagnetically stacked TLA [17]. It is well known for the latter that fluctuations lift the continuous degeneracy of the ground state in the presence of an in-plane field. Furthermore, the fluctuations stabilize collinear spin arrangements. Quantum Monte Carlo calculations for an XY-model with $S = 1/2$ predict three different types of spin structure to be stable in a transverse field: a chiral-ordered phase at low fields, a ferrimagnetic or collinear phase at intermediate fields, and a spin-flop-like 2–1 phase at high fields [18] (figure 10). The calculated phase diagram has much in common with the one determined for $CsCuCl_3$. Moreover, the calculated field dependence of the magnetization shows plateau-like behaviour for the intermediate phase and the IC1–IC3 transition always stays around $H_S/3$. However, one main quantitative difference between the model calculations and the case of $CsCuCl_3$ is the enlarged stability region for the IC3 phase at higher temperatures. As already pointed out, our measurements indicate a lifting of the frustration, i.e., the proportion of ordered moments increases with applied field. To our knowledge, these effects inherent to TLA systems have not yet been considered theoretically. Furthermore, it has to be noted that the situation is more complicated due to the presence of the Dzyaloshinskii–Moriya interaction for $CsCuCl_3$. For this system, elaborate calculations which include the effect of fluctuations at a phenomenological level by adding a biquadratic exchange to the energy were carried out in order to provide an understanding of the $M(H)$ and $Q(H)$ behaviour (the plateau in Q was reproduced) and the phase diagram, and to predict energetically favoured spin structures. It turned out that the results depend crucially on small anisotropies [5].

4. Conclusions

We have determined the phase diagram of the complex magnetic system $CsCuCl_3$ over a large temperature and field region. Our experimental results show a qualitative agreement of the

phase diagram of $CsCuCl_3$ with that predicted for the frustrated XY-model of a TLA with $S = 1/2$. The field independence of $Q(H)$ as well as the fixed intensity ratio of different Fourier components together with a plateau-like behaviour in $M(H)$ point to some locking of the magnetic structure for the IC3 phase at intermediate fields. The available data do not allow us to unambiguously distinguish between different models proposed for IC3. We tend to follow Nikuni's suggestion and think of domains of collinear or 2–1 arrangements separated along c by walls with large turning angles [14]. The ESR results [19,20] in the IC3 region with their many unexplained weak and strong resonances and the broadening of the neutron peaks support this picture. In addition, the domain effects seen in the asymmetric peak intensities (figure 7) apparently make 'chirality' visible for the first time using unpolarized neutrons. The commensurate phase probably consists of 2–1 domains (as shown in figure 9), with the result that the asymmetry evolves again when lowering the field and remains down to $H = 0$. To put these presumptions on a firmer basis, further diffraction experiments are planned.

Acknowledgment

We are indebted to K D Schotte for fruitful discussions.

References

[1] Hirotsu S 1977 *J. Phys. C: Solid State Phys.* **10** 967
[2] Adachi K, Achiwa N and Mekata M 1980 *J. Phys. Soc. Japan* **49** 545
[3] Nojiri H, Tokonuga Y and Motokawa M 1988 *J. Physique Suppl.* **49** C8 1459
[4] Nikuni T and Shiba H 1993 *J. Phys. Soc. Japan* **62** 3268
[5] Nikuni T and Jacobs A E 1998 *Phys. Rev.* B **57** 5205
[6] Jacobs A E and Nikuni T 1998 *J. Phys.: Condens. Matter* **10** 6405
[7] Jacobs A E, Nikuni T and Shiba H 1993 *J. Phys. Soc. Japan* **62** 4066
[8] Schotte U, Stüßer N, Schotte K D, Weinfurter H, Mayer H M and Winkelmann M 1994 *J. Phys.: Condens. Matter* **6** 10 105
[9] Watari S, Miyashita S and Shiba H 2001 *J. Phys. Soc. Japan* **70** 532
[10] Wolf B, Zherlitsyn S, Schmidt S and Lüthi B 1999 *Europhys. Lett.* **48** 182
[11] Bügel R, Faißt A, von Löhneysen H, Wosnitza J and Schotte U 2002 *Phys. Rev.* B **65** 052402
[12] Nojiri H, Takahashi T, Fukuda M, Fujita M, Arai M and Motokawa M 1998 *Physica* B **241–243** 210
[13] Schotte U, Kelnberger A, and Stüßer N 1998 *J. Phys.: Condens. Matter* **10** 6391
[14] Nikuni T 1995 *PhD Thesis* Tokyo Institute of Technology
[15] Dotsenko V S and Uimin G V 1985 *J. Phys. C: Solid State Phys.* **18** 5019
[16] Plakhty V P *et al* 2000 *Phys. Rev. Lett.* **85** 3942
[17] Chubukov A V and Golosov D I 1991 *J. Phys.: Condens. Matter* **3** 62
[18] Suzuki N and Matsubara F 1997 *Phys. Rev.* B **55** 12 331
[19] Schmidt S, Wolf B, Sieling M, Zvyagin S, Kouroudis I and Lüthi B 1998 *Solid State Commun.* **108** 509
[20] Ohta H, Imagawa S, Motokawa M and Tanaka H 1993 *J. Phys. Soc. Japan* **62** 3011